Label-free detection of Escherichia coli based on thermal transport through surface imprinted polymers.

Journal:	*ACS Sensors*
Manuscript ID	se-2016-00435x
Manuscript Type:	Article
Date Submitted by the Author:	13-Jul-2016
Complete List of Authors:	van Grinsven, Bart; Maastricht University, Maastricht Science Programme Eersels, Kasper; KULeuven, Physics and Astronomy, Soft Matter Physics and Biophysics Section Akkermans, Onno; Maastricht University, Maastricht Science Programme Ellermann, Sophie; Maastricht University, Maastricht Science Programme Kordek, Aleksandra; Maastricht University, Maastricht Science Programme Peeters, Marloes; Manchester Metropolitan University, Chemistry & Environmental Science Deschaume, Olivier; KU Leuven, Department of Physics and Astronom Bartic, Carmen; KU Leuven, Physics and Astronomy Diliën, Hanne; Maastricht University, Maastricht Science Programme Steen Redeker, Erik; Maastricht University, Maastricht Science Programme Wagner, Patrick; Katholieke Universiteit Leuven Faculteit Wetenschappen, Physics and Astronomy, Soft-matter Physics and Biophysics section Cleij, Thomas; Maastricht University, Maastricht Science Programme

Label-free detection of *Escherichia coli* based on thermal transport through surface imprinted polymers.

Bart van Grinsven[a*], Kasper Eersels[b], Onno Akkermans[a], Sophie Ellermann[a], Aleksandra Kordek[a], Marloes Peeters[c], Olivier Deschaume[b], Carmen Bartic[b], Hanne Diliën[a], Erik Steen Redeker[a], Patrick Wagner[b] and Thomas Cleij[a]

* = corresponding author

a) Maastricht University, Maastricht Science Programme, P.O. Box 616, 6200 MD Maastricht, The Netherlands.

b) KU Leuven, Soft-Matter Physics and Biophysics Section, Department of Physics and Astronomy, Celestijnenlaan 200 D, B-3001 Leuven, Belgium.

c) Faculty of Science and Engineering, School of Science and the Environment, Division of Chemistry and Environmental Science, Manchester Metropolitan University, Chester Street, Manchester M1 5GD, United Kingdom.

Keywords: Surface imprinted polymers, heat-transfer method (HTM), *Escherichia coli*, *Staphylococcus aureus*, point-of-care bacterial testing.

Abstract

This work focuses on the development of a label-free biomimetic sensor for the specific and selective detection of bacteria. The platform relies on the rebinding of bacteria to synthetic cell receptors, made by surface imprinting of polyurethane-coated aluminum chips. The heat-transfer resistance (R_{th}) of these so-called surface imprinted polymers (SIPs) was analyzed in

time using the heat-transfer method (HTM). Rebinding of target bacteria to the synthetic receptor led to a measurable increase in thermal resistance at the solid-liquid interface. *Escherichia coli* and *Staphylococcus aureus* were used as model organisms for several proof-of-principle experiments, demonstrating the potential of the proposed platform for point-of-care bacterial testing. The results of these experiments indicate that the sensor is able to selectively detect bacterial rebinding to the SIP surface, distinguishing between dead and living *E. coli* cells on the one hand and between Gram-positive and Gram-negative bacteria on the other hand (*E. coli* and *S. aureus*). In addition, the sensor was capable of quantifying the number of bacteria in a given sample, enabling detection at relatively low concentrations (10^4 CFU mL^{-1} range). As a first proof-of-application, the sensor was exposed to a mixed bacterial solution containing only a small amount (1%) of the target bacteria. The sample was able to detect this trace amount by using a simple gradual enrichment strategy.

Bacterial pathogens pose a major threat for public health care, causing a wide variety of conditions ranging from common illnesses to mortal infections. Adequate bacterial testing is therefore of major importance in various fields, including medicine (hospital-acquired infection, HAI), environmental and food safety (water-, air- and food-borne bacteria) and even counter-terrorism (Anthrax infection).[1] Food-borne pathogens cause an estimated 5000 deaths annually in the US alone,[2] while HAI's have shown to affect more than 1 in 20 people that are hospitalized in Florida.[3] The containment of bacterial infection is further complicated by the increasing number of multidrug-resistant bacteria, causing millions of deaths every year.[4]

Conventional diagnostic techniques are typically very slow and costly with a limited specificity and sensitivity. Samples are collected, labeled and analyzed in the lab by trained users using immunosorbent techniques such as ELISA.[5] More recently, sensitive molecular techniques have been developed that are able to selectively detect bacteria in a faster manner. These techniques make use of genetic screening, PCR or real-time PCR and are a huge improvement in comparison to the more classical techniques but they still require sample preparation and expensive equipment that needs to be used in a lab environment by skilled personnel, limiting their use in point-of-care applications.[6-8] Therefore, a reliable test that can be used "on-the-bench" could lead to a more accurate and faster diagnosis, thereby improving the prognosis for the patient.

Biosensors offer an elegant alternative to these expensive techniques as they are typically fast, cost-effective and label-free and therefore more suitable for point-of-care applications. Various biosensor platforms have been developed for bacterial identification. These devices employ numerous transducer mechanisms including impedance spectroscopy,[9-11] optical detection,[12-14] and microgravimetry.[15-17] Although these devices are very sensitive and selective and overcome the problem associated with more expensive, complicated techniques,

there are some drawbacks associated with their use. Biosensors rely on biological receptors such as antibodies,[18, 19] bacteriophages[20] or aptamers[21] to detect their target. Although these receptors display a high affinity for their target they can be disadvantageous in terms of stability and the complex nature of their synthesis procedure.

The use of synthetic receptors might overcome the problems associated with the use of natural receptors in sensor applications. Synthetic receptors made by molecular imprinting mimic the target sensitivity and selectivity of an enzyme[22] but are more stable, reusable, easier and cheaper to produce and have an unlimited shelf-life.[23] Over the past two decades, the concept of molecular imprinting has been extended towards surface imprinting of thin polymer layers for macromolecular templates using various imprinting approaches.[24-28] Surface-imprinted polymers (SIPs) have been incorporated into numerous biomimetic sensor applications. Platforms based on optical techniques such as ELISA, confocal and fluorescence microscopy have proven to be very selective and extremely sensitive.[29-33] However, since these techniques rely on expensive equipment, operated by experienced users in a lab environment and are difficult to miniaturize their applicability for point-of-care testing is limited. Therefore, label-free, low-cost alternatives have been developed based on classical biosensor read-out platforms based on microgravimetrical,[34-36] electrochemical,[37-39] and optical detection principles.[40-42]

In this article, the authors present a new platform for bacterial detection based on the heat-transfer method (HTM). This read-out technique has proven to be a versatile tool for biosensing[43] and was combined with SIPs in a biomimetic assay for the detection of cancer cells.[44-46] Due to its relatively simple and low-cost nature, HTM offers several benefits over classical biosensing techniques. Impedance spectroscopy, quartz crystal microbalances and surface plasmon resonance *f.e.* require some degree of temperature control, in addition to the sensing hardware, to function optimally. HTM on the other hand, requires little

instrumentation as it functions as a sensing and temperature control platform at the same time which limits the cost price of the device. Additionally, the data interpretation is relatively straightforward and the device can be easily scaled down in terms of point-of-care sensing. Furthermore, HTM does not rely on the electrical conductivity or piezoelectric properties of the platform material, any solid material can be used as platform provided that it does not inhibit the heat flow through the SIP layer.

In this paper, polyurethane-coated aluminum chips were imprinted with *Escherichia coli* and *Staphylococcus aureus* by the so-called micro-contact printing approach that was previously developed by Dickert *et al*.[27, 47] Rebinding of bacteria to the SIP lead to a measurable increase in thermal resistance, detected by HTM. In order to establish a proof-of-principle, it was assessed whether or not the sensor was able to distinguish between living and dead bacteria and could selectively detect *E. coli* and *S. aureus*. Additionally, a limit of detection (LoD) was determined and a first proof-of-application was demonstrated, detecting a trace amount of *E. coli* (1 %) in the presence of an excess of *S. aureus*.

Experimental Methods

Bacterial culturing and sample preparation The characterized strains of *Escherichia coli* (ATCC® 8739™) and *Staphylococcus aureus* (ATCC® 6538™) were obtained from DSM-Z. 20 ml nutrient broth (NB, x929.1 ROTH) and Caso broth (TSB, x938.1 ROTH) were inoculated with a single colony of E. coli and S. aureus respectively and allowed to grow overnight at 37°C while shaking. Prior to imprinting, 1ml of the overnight culture was diluted in 20 ml of the respective broth, and allowed to grow at 37°C for 3 hours or until OD600 of 1 was obtained. Afterwards, the cells were harvested by centrifugation and the pellets were washed one time with PBS, and resuspended in phosphate buffered saline to achieve the desired concentration.

Preparation of bacteria-imprinted polyurethane layers Polyurethane layers were synthesized by dissolving 122 mg of 4,4′-diisocyanatodiphenylmethane, 222 mg of bisphenol A, and 25 mg of phloroglucinol in 500 μL of anhydrous tetrahydrofuran (THF). All reagents had a purity of at least 99.9% and were used as received (Sigma-Aldrich N.V., Diegem, Belgium). The mixture was polymerized up to the gelling point at 65°C for 200 minutes while gently stirring. The solution was diluted in anhydrous THF in a 1:5 ratio. Polyurethane layers with an an average thickness of 1.2 ± 0.1 μm, as measured with a profilometer (Dektak3ST, Sloan Instruments Corporation, Santa Barbara, CA) were created by spincoating the solution during 60 s at 2000 rpm onto 1 cm^2 aluminum substrates.

In parallel, bacteria-covered homemade polydimethylsiloxane (PDMS) stamps were formed by applying 400 μL of a bacterial suspension in PBS to the stamp. The bacteria were allowed to sediment to the surface of the stamp for 10 minutes and the excess fluid was removed by spin coating the stamp at 3000 rpm for 60 s to create a dense monolayer of bacteria on the stamp surface. PDMS stamps were made using the Sylgard 184 silicone elastomer kit (Malvom N.V., Schelle, Belgium). The bacteria-covered stamps were gently pressed onto the semi-cured polyurethane layer to ensure full contact and the bacteria were allowed to sink into the layer passively due to the weight of the stamp. Finally, the polymer was cured for 18 hours at 65°C under inert atmosphere after which the stamp was removed from the surface. Template bacteria were washed off with a 70 % ethanol in MilliQ and PBS, leaving behind selective binding cavities on the surface, creating SIPs for *E. Coli* and *S. aureus*.

Sensor setup & measuring methodology The sensor setup and its use in cell-binding assays has been described earlier.[34-37] The proportional-integral-derivative (PID) settings (P = 1, I = 8, D = 0) used were optimized in a previous study.[38] The system is allowed to stabilize in PBS

buffer (pH = 7.4) at the beginning of each experiment. Bacteria are introduced to the system by injecting 3 mL of a bacterial solution (1×10^7 CFU mL^{-1} in PBS) at a controlled flow rate of 2.5 mL min^{-1}. The system is left to stabilize after which the system is flushed with PBS at a flow rate of 0.25 mL min^{-1} for 12 minutes (total volume 3 mL) to remove any unbound bacteria from the SIP layer. The HTM setup monitors the thermal resistance (R_{th}) at the solid-liquid interface at a rate of one measurement per second.

Imprint characterization Microscopic imaging of the cell-imprinted polyurethane surfaces was performed with a Leica DM750 optical microscope (Leica Microsystems, Diegem, Belgium. All SIPs were imaged at magnifications 640x and 1000x. ImageJ 1.44P (National Institute of Health, Bethesda, MA, USA) was used to determine the number of cell imprints per area unit on microscopic images of the SIPs. The average surface coverage of cell imprints on the polyurethane layer was calculated based on cell imprint counts of three different samples for each type of SIP and five locations on each sample. An Agilent 5500 AFM system was used with MSNL-F cantilevers (f = 110=120 kHz, k = 0.6 N/m) with average tip radius of 2=12 nm for topographical imaging in intermittent contact (AAC) mode. The AFM topography images were leveled, line-corrected and measured (height profiles) using Gwyddion, a free and open-source SPM (scanning probe microscopy) data visualization and analysis program.

Results

Surface characterization and calculation surface coverage Optical analysis of a SIP surface imprinted with *E. coli* clearly reveals a heterogeneous distribution of imprints with an average diameter of 0.5 to 2 µm, corresponding to the dimensions of the template bacteria (figure 1a). The calculated surface coverage of $7.18 \times 10^6 \pm 8.54 \times 10^5$ imprints cm^2 corresponds to a total surface coverage of 14.13 ± 1.8 %. The microscopic analysis of the *S.*

aureus SIP (figure 1b) shows a heterogeneous distribution of spherical imprints with a diameter of ± 500 nm – 800 nm. The imprint surface coverage of $5.82 \times 10^6 \pm 9.84 \times 10^5$ imprints cm^2 corresponds to a total surface coverage of 12.36 ± 2.3 %.

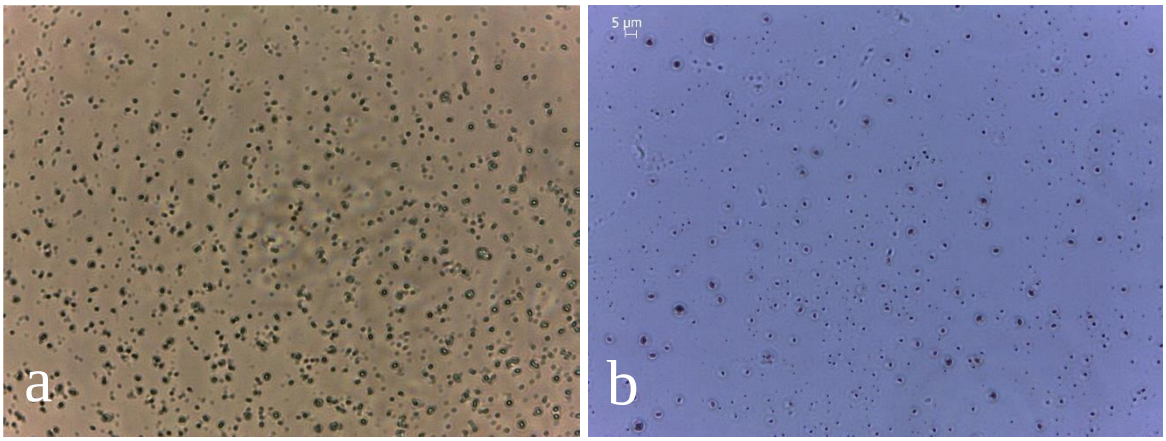

Figure 1. Microscopic analysis of an *E. coli* (a) and *S. aureus* SIP (b). Images were made at a magnification of 1000 and Image J was used to calculate imprint surface coverage.

To analyze the morphology of the imprints more thoroughly, an *E. coli* SIP was used for topographical analysis with an atomic force microscope (Figure 2). The overview of a 20 x 20 µm2 area clearly shows a heterogeneous distribution of rod-shaped imprints with lengths ranging from 0.5 to 2 µm and widths of 0.2-0.5 µm which corresponds well to the shape and size of the template bacteria (figure 2a). One of these imprints was analyzed more thoroughly confirming that the horizontal dimensions of the template are faithfully transferred into the SIP layer (figure 2b). However, the 3D image and depth profile (figure 2c and d) indicate that the vertical dimensions are not transferred to the layer, as the imprint is quite shallow ranging up to about 30-40 nm in depth. These data are in accordance with a previously performed analysis on a MCF-7 SIP which demonstrated that the shallow nature of the imprints is actually the key to their selectivity.[44]

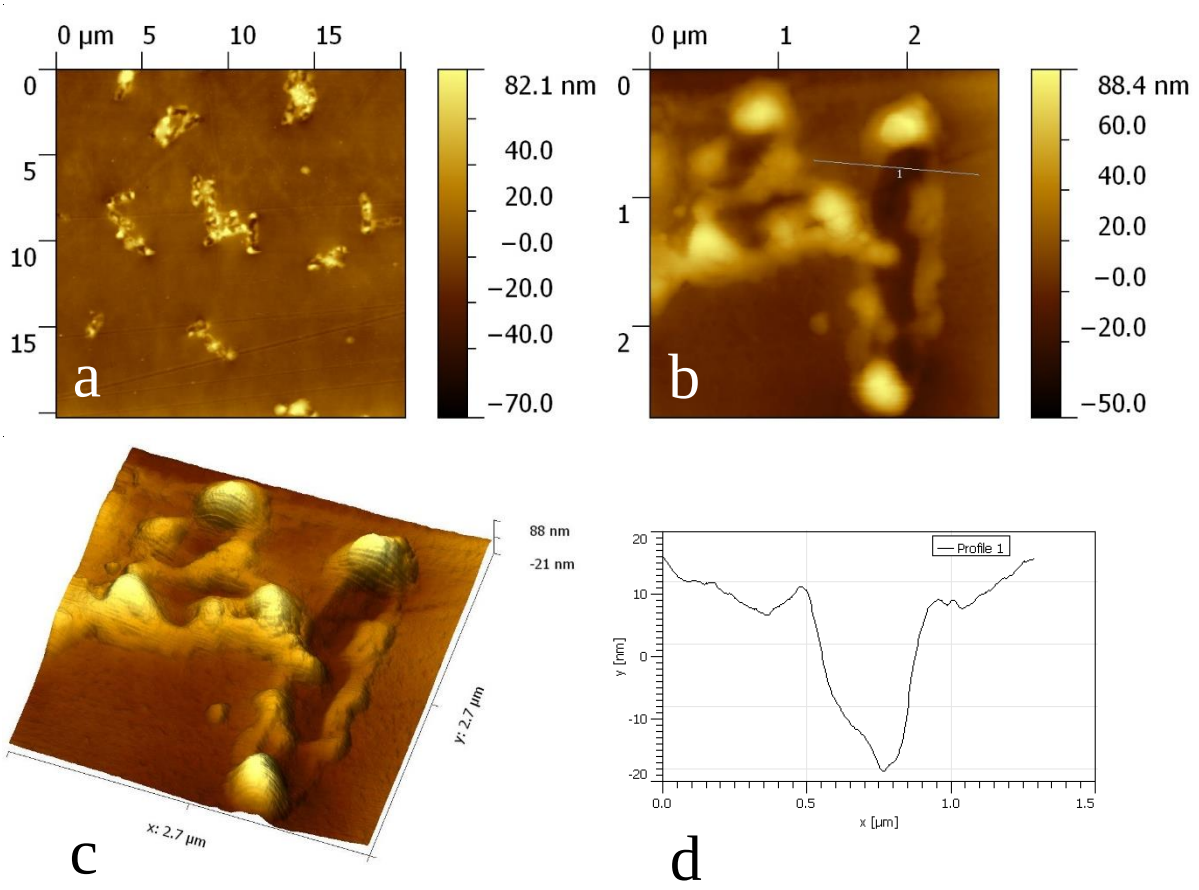

Figure 2. Topographical analysis of an E. coli SIP using an atomic force microscope. Rod-size imprints can be observed (a) with dimensions corresponding well to the size and shape of the template bacteria (b). The 3D-imprint (c) and depth (d) profile reveal that the imprints are quite shallow with depths up to 40 nm.

Bacterial detection and live/dead discrimination The setup's potential to discriminate between living and dead bacteria, SIP's were imprinted with living *E. coli* cells in PBS (concentration 1×10^7 CFU mL^{-1}) as described in Experimental Section 2.2. The SIP-coated aluminum was mechanically pressed with its non-coated, polished backside onto a copper block, ensuring an optimal thermal contact between chip and heat sink. The flow cell was filled with PBS and the R_{th} signal was allowed to stabilize for 60 minutes.

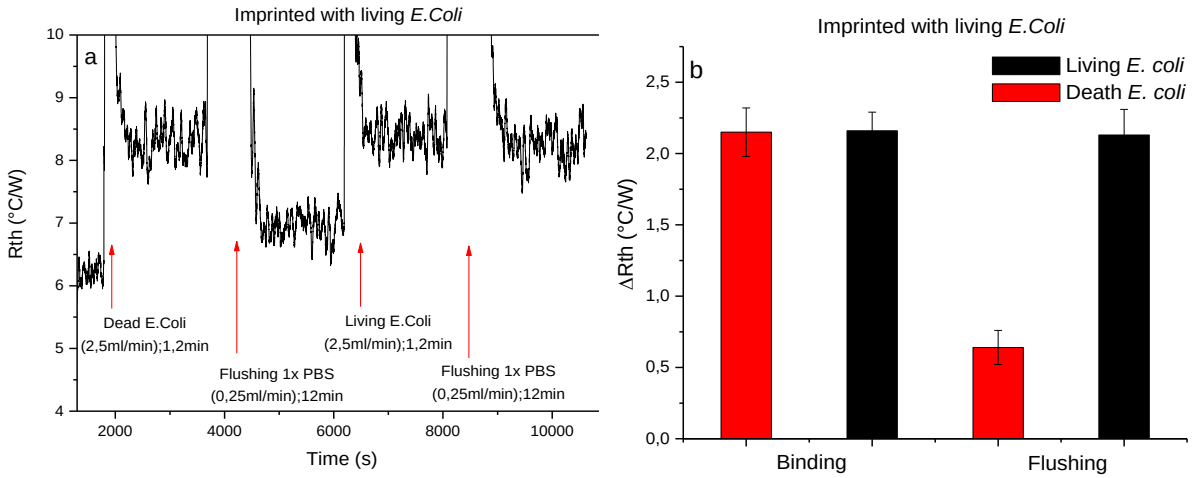

Figure 3. Time-dependent R_{th} data of a SIP imprinted with living *E. coli* cells after consecutive exposure to PBS solutions containing dead and live *E. coli* respectively (1×10^7 CFU mL^{-1}) (a). The results demonstrate that both exposure events result in an increase in thermal resistance at the solid-liquid interface. The increase associated with an addition of dead bacteria can be partially reversed by flushing with PBS, whereas the increase caused by adding living *E. coli* cells is irreversible. A boxplot is shown summarizing the data (b). Error bars indicate the standard deviation of the noise on the signal.

Dead bacteria are introduced into the flow cell at a flow rate of 2.5 mL min^{-1} (72 seconds, 3mL). The flow is stopped and the signal is left to stabilize for 60 minutes, allowing the bacteria to sediment towards the SIP surface. Any unbound bacteria are removed by flushing the flow cell with PBS at a rate of 0.25 mL min^{-1} (12 minutes, 3mL). After a 60-minute stabilization interval, the experiment is repeated with living *E. coli* cells. The results of this experiment are shown in figure 3 and demonstrate that the signal increases upon addition of a solution of dead bacteria in PBS by 2.15 ± 0.17 °C/W. Upon flushing the chamber with PBS the signal drops back with to a value 0.64 ± 0.12 °C/W above the baseline. After infusing the live bacteria into the measuring chamber the signal increases again to a value 2.16 ± 0.13

°C/W. Flushing with buffer solution does not cause a measurable decrease in R_{th} as the signal remains at 2.13 ± 0.18 °C/W above the baseline.

Selectivity test: *E. coli* (Gram-negative) vs. *S. aureus* (Gram-positive) To investigate the selectivity of the proposed platform, SIP's were imprinted with *S. aureus* and *E. coli* analogous to the experiment described in Section 3.2. The time-dependent R_{th} data acquired by consecutively exposing the SIP's to analogue non-target bacteria and target bacteria. The flow cell is flushed at a controlled velocity between both exposure events.

The data summarized in figure 4a indicate that exposing an *E. coli* SIP to a suspension of *S. aureus* cells in PBS (concentration 1×10^7 CFU mL^{-1}) increases the thermal resistance at the solid-liquid interface with 1.91 ± 0.22 °C/W. Rinsing the flow cell with PBS will return the signal back to baseline (ΔR_{th} = 0.06 ± 0.15 °C/W). Repeating the cycle with an *E. coli* solution with the same concentration will lead to an irreversible increase in R_{th} of 2.13 ± 0.14 °C/W (ΔR_{th} upon flushing = 2.08 ± 0.23 °C/W). A similar trend can be observed when performing the same experiment with a *S. aureus* SIP (figure 4b). Exposure to a solution of *E. coli* cells increases the R_{th} signal with 1.63 ± 0.15 °C/W but upon rinsing the flow cell with PBS the thermal resistance stabilizes at a value -0.14 ± 0.25 °C/W above the baseline. Exposing the SIP to a solution of target cells on the other hand, will lead to an increase in thermal resistance of 1.79 ± 0.14 °C/W. Flushing the cell with PBS will not significantly change the signal (1.77 ± 0.16 °C/W).

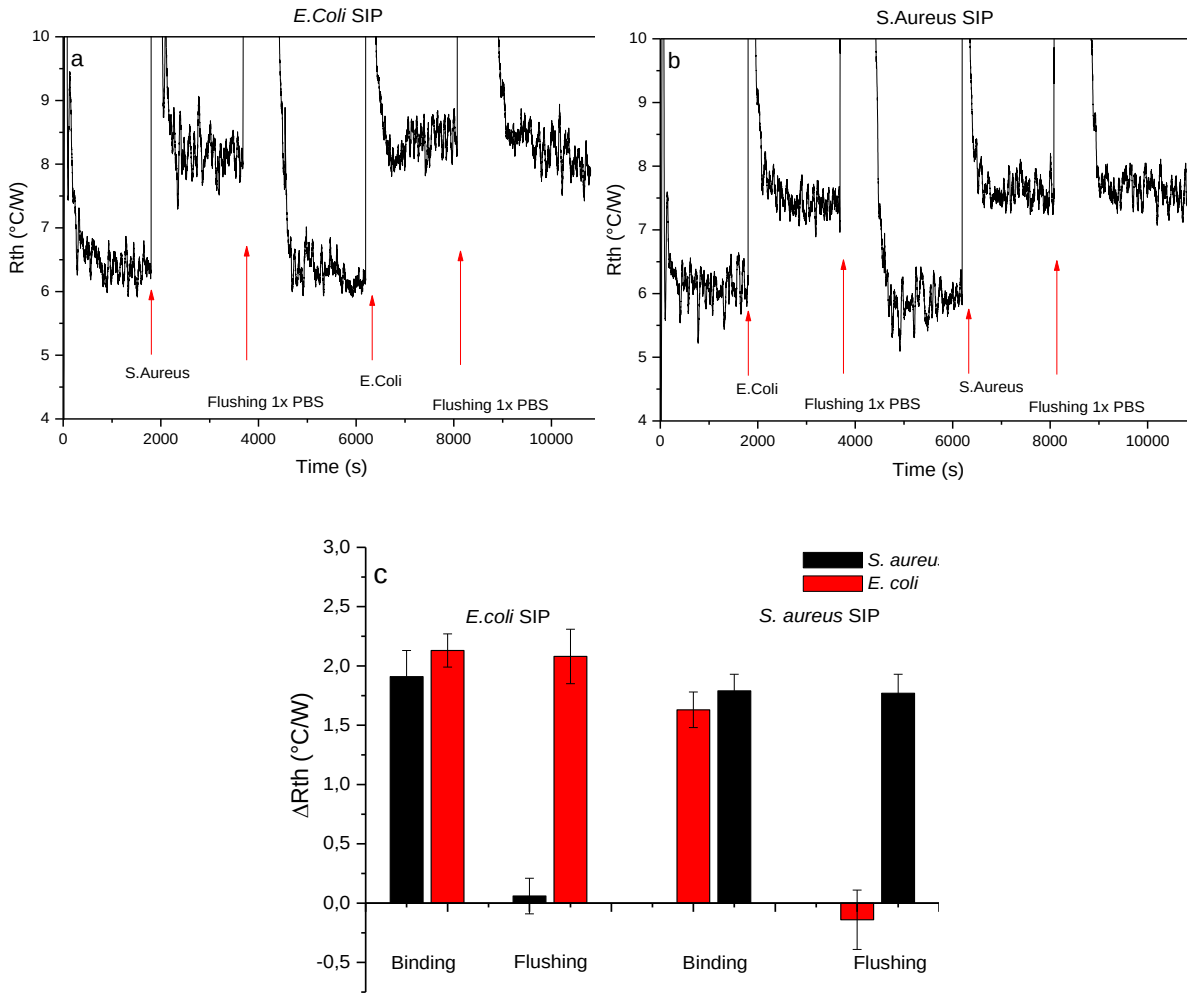

Figure 4. Time-dependent R_{th} measurements of SIPs imprinted with either *E. coli* (a) or S. *aureus* (b) during consecutive bacterial exposure events to analogue non-target bacteria and finally target bacteria. In both cases, addition of non-target bacterial species leads to an increase in thermal resistance, but the signal returns back to baseline upon flushing the flow cell with buffer solution. Binding of target bacteria to the SIP on the other hand, leads to an irreversible rise in R_{th}. The results of this experiment are summarized in a box plot (c).

Sensitivity test: dose-response curve In order to determine the limit-of-detection (LoD) of the sensor, the time-dependent R_{th} response of an *E. coli* SIP, exposed to an increasing concentration of target cells, was analyzed. To this extent a stock solution of *E. coli* cells in PBS with a concentration of 1×10^{7} CFU mL^{-1} was diluted 1000, 500, 200, 100, 50, 20, 10 and

5 times and the SIP was consecutively exposed to an increasing concentration of target cells. In between each exposure step, the flow cell is rinsed with ethanol and, upon stabilization of the signal, PBS to ensure full removal of the bacteria from the SIP layer both steps were performed at a rate of 0.25 mL min^{-1} (12 minutes, 3mL). The results of this experiment are described in figure 5.

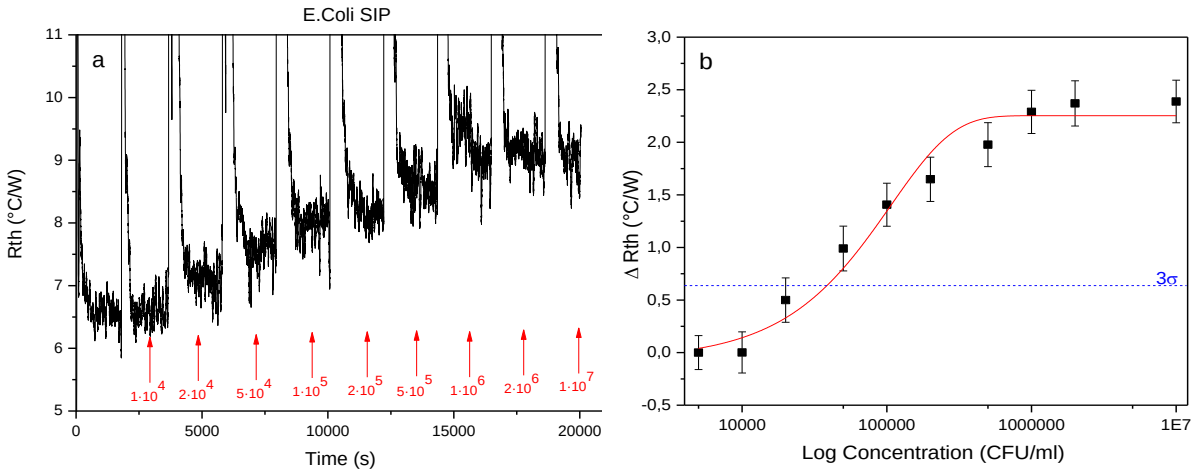

Figure 5. Dose-response experiment performed on a SIP imprinted with *E. coli*. A stock solution (1×10^7 CFU mL^{-1}) was diluted 1000, 500, 200, 100, 50, 20, 10 and 5 times and the SIP was exposed to an increasing concentration of target cells (a). Upon each exposure step, the layer was rinsed with ethanol and PBS to ensure full removal of the cells. The thermal resistance increases noticeably and the increase seems to be concentration-dependent. These results combined with the results from the previous experiment were used to establish a dose-response curve: response in R_{th} as a function of the added target-bacteria concentration (logarithmic). An exponential fit is drawn trough the obtained data with an R^2-value of 0.97. The dashed line corresponds to the limit-of-detection, defined as three times the highest error on the data (b).

The time-dependent thermal resistance data shown in figure 5a, indicate that exposing the SIP to a concentration of 1×10^4 CFU mL^{-1} does not result in a measurable increase in R_{th}. Upon

addition of a concentration of 2×10^4 CFU mL^{-1} the signal starts increasing in a concentration-dependent manner and saturates at a concentration of 2×10^6 CFU mL^{-1}. These data were used to obtain a dose-response curve (figure 5b). The dose-response curve nicely follows ($R^2 = 0.97$) an empirical, exponential fit function according to the formula:

$$\Delta Rth(c) = A - B \bullet \exp\{-\frac{c}{C}\}$$

The limit-of-detection was calculated using this dose-response curve and is defined as the intercept between the fitted curve and the dashed line in figure 5b corresponding to three times the biggest error on the data set.[44]

Proof-of-application: detection of *E. coli* in a semi-complex matrix The results obtained in the previous sections indicate that the sensor is indeed able to selectively and specifically detect bacterial cells in buffer. To examine if our sensor is able to detect its target in a more complex matrix a mixed cell solution was made containing both *E. coli* and *S. aureus* cells in a 1:99 ratio (total concentration of bacteria: 1×10^7 CFU mL^{-1}). This mixture was used in a progressive enrichment experiment, exposing a SIP imprinted with *E. coli* three consecutive times to the mixture, while flushing the layer with buffer between each exposure event. The results are shown in figure 6 and indicate that the signal does not significantly increase in comparison to the baseline after the first exposure event. The net change in thermal resistance appears to be positively correlated to the number of exposure steps as R_{th} increases after the second and third exposure step.

To demonstrate this effect more clearly, the saturation level at each step was determined as the ratio of ΔR_{th} after exposure to the mixture and after flushing with buffer respectively. The LoD is illustrated as a dashed line and is defined as three times the standard deviation on the signal corresponding to 26.424 %. After the first two cycles the signal only reaches 0.8 ± 8.08

% and 11.8 ± 7.82 %, well below the detection limit. After a third exposure round the signal reaches the limit of detection at a saturation level of 32.1 ± 8.00 %.

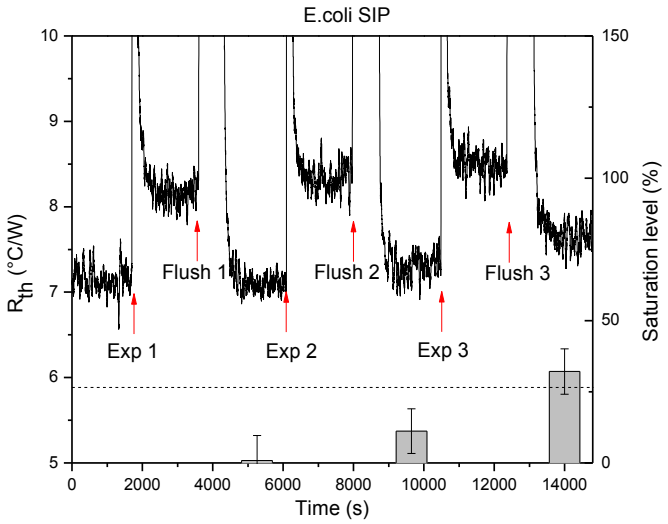

Figure 6. Progressive enrichment experiment conducted on an aluminum chip covered with an *E. coli* SIP. The SIP is exposed to a 1:99 mixture of *E. coli* and *S. aureus* cells. Each exposure event consists of injection of the mixture, stabilization of the signal, rinsing the flow cell with buffer and another stabilization period. This cycle is repeated three consecutive times. The data show that the signal gradually increases after each exposure event. This was summarized in a box plot of the saturation level, defined as the ratio of ΔR_{th} after flushing and exposure respectively. The dashed line corresponds to the LoD, defined as three times the standard error on the signal.

Discussion

The experiments on dead and living *E. coli* cells clearly demonstrate that the difference in surface chemistry is sufficiently big to discriminate between both, despite the morphological similarities. The thermal resistance profile in figure 3 shows a comparable response upon initial exposure to dead and living bacteria, although the increase in R_{th} is somewhat lower for dead cells. This can be explained by the fact that the morphology of the dead cells is compatible to the dimensions of the microcavities on the SIP surface. Both living and dead

cells block the heat flow through the microcavities of the SIP, thereby increasing the heat-transfer resistance at the solid-liquid interface. However, as the AFM analysis in figure 2 demonstrates that the imprints are quite shallow in comparison to the diameter of the template, which corresponds to previous findings,[44] the morphological match must be complemented by a complementarity in the distribution of functional groups between imprint and template to ensure tight adhesion of bacteria to the surface. Previous research has demonstrated that both protein expression and the presence of carbohydrate groups on the outer membrane of the cells are decisive elements in the recognition of cells by SIPs.[45] In addition, Hayden *et al.* demonstrated that the recognition is driven by the formation of hydrogen bonds that were created between imprint and template during crosslinking of the polymer in the imprinting procedure.[35] This explains why the signal returns back to baseline after flushing with PBS in the exposure experiment performed with the dead *E. coli* cells. The bacteria were killed in 70% ethanol which denatures the membrane proteins of the cells and dissolves the phospholipids inside the membrane. Therefore, the dead bacteria are not tightly bound to the SIP and can be washed out easily. The small degree of cross-selectivity that is observed can be attributed to the fact that some carbohydrate patterns might still be present on the dead cells which, by chance, might result in a bond that is strong enough to withstand the shear force associated with flushing.

The cross selectivity experiment described in figure 4 reveals a similar trend. In both cases, exposure of the SIP to a solution containing an analogue bacterial species, leads to an increase in thermal resistance. However, these cells can be washed away easily by rinsing the flow cell with PBS, while target cells remain bound to the layer, even after flushing. This can be explained the fact that gram-negative *E. coli* and gram-positive *S. aureus* have a distinctly different outer membrane in terms of protein expression and the presence of carbohydrate patterns.[48, 49] The bond between the analogue cells and the SIP can therefore be easily broken

by flushing the flow cell with buffer. The target bacteria on the other hand, remain firmly bound to the layer and the thermal resistance remains at an elevated level even after flushing.

The data in figure 5 reveal that the sensor does not only qualitatively respond to an elevated concentration of target bacterial species in a sample but the response can also be quantified. At relatively low concentrations, the sensor's response stays within noise levels and can therefore not be regarded as significant. But starting from a concentration of 2×10^4 CFU mL^{-1} we see the signal significantly increasing to a value well above the baseline, indicating that a sufficient amount of cells interacts with and binds to the microcavities on the SIP, blocking the heat flow through the layer and thereby increasing the heat-transfer resistance. This effect becomes more pronounced with an increasing concentration but the sensor seems to saturate at concentrations above 2×10^6 CFU mL^{-1}. Using the exponential fit to the data and defining the detection limit as the concentration at which the signal-to-noise ratio is bigger than 3, we calculated the LoD at 3.5×10^4 CFU mL^{-1}. Although there are label-free platforms that are more sensitive,[1] HTM has the benefit of being very low-cost, user-friendly and can be easily scaled down in terms of point-of-care sensing. Furthermore, all data shown are raw, unfiltered data. The amount of noise on the signal that can be observed, originates from stringently controlling the temperature underneath the sample (T_1). However, the noise can be decreased by filtering, electronic noise reduction and careful re-designing of both the flow cell and the measuring device, which would significantly improve the sensitivity of the set up. The experiments demonstrated in this article describe a very first series of experiments that assess the platform's potential for bacterial identification.

The final set of experiments provides a very first proof-of-application illustrating how the sensor would respond to a more complex matrix as opposed to a cell solution containing only one type of bacterial species. The results in figure 6 also demonstrate another possible method for improving the LoD by gradually exposing the SIP to target cells during multiple

consecutive exposure cycles. After exposure to the bacterial mixture, the R_{th} signal initially increases to saturation which indicates that both target and analogue cells bind to the layer. After flushing the signal falls back to a value that does not significantly differ from the baseline value. This can be explained by the fact the *E. coli* cells are overwhelmed by a 99-fold excess of *S. aureus* cells which also bind to the microcavities upon addition of the mixture to the flow cell. *E. coli* cells cannot bind to microcavities that are already occupied by analogue bacteria. Due to steric hindrance the analogue bacteria also prevent the target bacteria from interacting with the SIP. These findings indicate that the sensitivity of the platform could decrease when analyzing bacteria in a complex matrix. This can be overcome by increasing the number of exposure cycles. With this enrichment strategy, the signal will gradually increase with each cycle and eventually reach the LoD which enables detection of lower concentrations of bacteria in increasingly complex mixtures. In order to detect trace amounts of bacteria in biological or environmental samples the device will need to be redesigned and probably combined with pretreatment of the samples under analysis.

Conclusion

The results obtained during this study indicate that the proposed sensor platform is able to detect bacteria in buffer with a high degree of selectivity. Although the device performance has only been assessed in buffer the presented manuscript offers a first proof-of-principle, illustrating the potential of the combination of SIP's and HTM for bacterial detection. Further research should be devoted at improving the sensitivity of the device. This can be achieved by optimizing the imprinting procedure to obtain a higher and more homogenous surface coverage on the SIP surface which will lead to a larger effect size and improved LoD. In addition, the noise on the thermal resistance signal can be improved by optimizing both the measurement technique and flow cell. Finally, the results obtained within, the gradual

enrichment experiment indicate that the sensitivity of the device can be improved by maximizing the exposure between sample and receptor layer by *e.g.* developing a flow cell for continuous exposure.

Author Information

Corresponding author

Dr. Bart van Grinsven. Present address: Maastricht University, Maastricht Science Programme, P.O. Box 616, 6200 MD, Maastricht, the Netherlands. Tel.: 0031/(0)6.39.60.22.89, Email: bart.vangrinsven@maastrichtuniveristy.nl

Author Contributions

B.v.G. and K.E. contributed equally to this work. K.E. prepared all cell-imprinted polymer layers and was responsible for culturing cells in cooperation with O.A. and E.S.R. O.A., S.E. and A.K. were in charge of optical analysis of the surface. The heat-transfer device was designed and built by B.v.G, H.D. and T.J.C. All heat-transfer measurements were performed by B.v.G. in cooperation with K.E and O.A. Biological assistance and guidance on possible medical/biotechnological applications was provided by S.E., A.K., E.S.R. and P.W., while H.D., M.P. and T.J.C. provided input on SIP synthesis and template removal. B.v.G. and K.E. interpreted the heat-transfer data in close cooperation with T.J.C. and P.W. O.D. and C.B. performed the AFM analysis on the samples and assisted in interpreting the results. The manuscript was jointly written by K.E. and B.v.G. All authors have given approval to the final version of the manuscript.

Acknowledgements

This work was financed by the Maastricht Science Programme of Maastricht University and the C1 project “Smart Cellular Scaffolds” from KU Leuven (C14/15/067). Technical support by I. Muijrers-Chen, W. Stilman and J. Dassen was greatly appreciated.

References

(1) Ahmed, A.; Rushworth, J.V.; Hirst, N.A.; Milner, P.A. Biosensors for Whole-Cell Bacterial Detection. Clin. Microbiol. Rev. **2014**, 27, 631-645.

(2) Scallan, E.; Hoekstra, R.M.; Angulo, F.J.; Tauxe, R.V.; Widdowson, M.A.; Roy, S.L.; Jones, J.L.; Griffin, P.M. Foodborne Illness Acquired in the United States – Major Pathogens. *Emerg. Infect. Dis.* **2011**, 17, 7-15.

(3) Magill, S.S.; Hellinger, W.; Cohen, J.; Kay, R.; Bailey, C.; Boland, B.; Carey, D.; de Guzman, J.; Dominguez, K.; Edwards, J.; Goraczewski, L.; Horan, T.; Miller, M.; Phelps, M.; Saltford, R.; Seibert, J.; Smith, B.; Starling, P.; Viergutz, B.; Walsh, K.; Rathore, M.; Guzman, N.; Fridkin, S. Prevalence of Healthcare-Associated Infections in Acute Care Hospitals in Jacksonville, Florida. *Infect. Control Hosp. Epidemiol.* **2012**, 33, 283-291.

(4) Nikaido, H. Multidrug Resistance in Bacteria. *Annu Rev Biochem.* **2009**, 78: 119–146.

(5) Fournier, P..; Drancourt, M.; Colson, P.; Rolain, J.; Scola, B.L.; Raoult, D. Modern Clinical Microbiology: New Challenges and Solutions. Nat. Rev. Microbiol. **2013**, 11, 574-585.

(6) Croxen, M.A.; Law, R.J.; Scholz, R.; Keeney, K.M.; Wlodarska, M.; Finlay, B.B. Recent Advances in Understanding Enteric Pathogenic Escherichia Coli. *Clin. Microbiol. Rev.* **2013**, 26, 822-880.

(7) Burnham, C.A.; Carroll, K.C. Diagnosis of Clostridium Difficile Infection: An Ongoing Conundrum for Clinicians and for Clinical Laboratories. *Clin. Microbiol. Rev.* **2013**, 26, 604-630.

(8) Espy, M.J.; Uhl, J.R.; Sloan, L.M. Buckwalter, S.P.; Jones, M.F.; Vetter, E.A.; Yao, J.D.; Wengenack N.L.; Rosenblatt, J.E.; Cockerill III, F.R.; Smith, T.F. Real-Time PCR in Clinical Microbiology: Applications for Routine Laboratory Testing. *Clin. Microbiol. Rev.* **2006**, 19, 165-256.

(9) Maalouf, R.; Fournier-Wirth, C.; Coste, J.; Chebib, H.; Saikali, Y.; Vittori, O.; Errachid, A.; Cloarec, J.P.; Martelet, C.; Jaffrezic-Renault, N. Label-Free Detection of Bacteria by Electrochemical Impedance Spectroscopy: Comparison to Surface Plasmon Resonance. *Anal. Chem.* **2007**, 79, 4879-4886.

(10) de la Rica, R.; Baldi, A.; Fernandez-Sanchez, C.; Matsui, H. Selective Detection of Live Pathogens via Surface-Confined Field Perturbations on Interdigitated Silicon Transducers. *Anal. Chem.* **2009**, 81, 3830-3835.

(11) Guo, X.F.; Kulkarni, A.; Doepke, A.; Halsall, H.B.; Iyer, S.; Heineman, W.R. Carbohydrate-Based Label-Free Detection of Escherichia coli ORN 178 Using Electrochemical Spectroscopy. *Anal. Chem.* **2012**, 84, 241-246.

(12) Ohk, S.H.; Koo, O.K.; Sen, T.; Yamamoto, C.M.; Bhunia, A.K. Antibody-Aptamer Functionalized Fibre-Optic Biosensor for Specific Detection of Listeria Monocytogenes From Food. *J. Appl. Microbiol.* **2010**, 109, 808-817.

(13) Wang, Y.; Knoll, W.; Dostalek, J. Bacterial Pathogen Surface Plasmon Resonance Biosensor Advanced By Long Range Surface Plasmons and Magnetic Nanoparticle Assays. *Anal. Chem.* **2012**, 84, 8345-8350.

(14) Tripathi, S.M.; Bock, W.J.; Mikulic, P.; Chinnappan, R.; Ng, A.; Tolba, M.; Zourob, M. Long Period Grating Based Biosensor for the Detection of Escherichia Coli Bacteria. *Biosens. Bioelectron.* **2012**, 35, 308-312.

(15) Hao, R.; Wang, D.; Zhang Xe Zuo, G.; Wei, H.; Yang, R.; Zhang, Z.; Cheng, Z.; Guo, Y.; Cui, Z.; Zhou, Y. Rapid Detection of Bacillus Anthracis Using Monoclonal Antibody Functionalized QCM Sensor. *Biosens. Bioelectron*. **2009**, 24, 1330-1335.

(16) Jiang, X.; Wang, R.; Wang, Y.; Su, X.; Ying, Y.; Wang, J.; Li, Y. Evaluation of Different Micro/Nanobeads Used as Amplifiers in QCM Immunosensor for More Sensitive Detection of E. Coli O157:H7N. *Biosens. Bioelectron*. **2011**, 29, 23-28.

(17) Salam, F.; Uludag, Y.; Tothill, I.E. Real-Time and Sensitive Detection of Salmonella Typhimurium Using an Automated Quartz Crystal Microbalance (QCM) Instrument with Nanoparticles Amplification. *Talanta* **2013**, 115, 761-767.

(18) Liger, F.S.; Sapsford, K.E.; Golden, J.P. Shriver-Lake, L.C.; Taitt, C.R.; Dyer, M.A.; Barone, S.; Myatt, C.J. The Array Biosensor: Portable, Automated Systems. *Anal. Sci.* **2007**, 23, 5-10.

(19) Joung, C-K.; Kim, H-N.; Im, H-C.; Kim, H-Y.; Oh, M-H.; Kim, Y-R. Ultra-Sensitive Detection of Pathogenic Microorganism Using Surface-Engineered Impedimetric Immunosensor. *Sensor. Actuat. B-Chem.* **2012**, 161, 824-831.

(20) Neufeld, T.; Schwartz-Mittelmann, A.; Biran, D.; Ron, E.Z.; Rishpon, J. Combined Phage Typing and Amperometric Detection of Released Enzymatic Activity for the Specific Identification and Quantification of Bacteria. *Anal. Chem.* **2003**, 75, 580-585.

(21) Zelade-Guillen, G.A.; Sebastian-Avila, J.L.; Blondeau, P.; Riu, J.; Rius, F.X. Label-Free Detection of Staphylococcus Aureus in Skin Using Real-Time Potentiometric Biosensor Based on Carbon Nanotubes and Aptamers. *Biosens. Bioelectron.* **2012**, 31, 226-232.

(22) Mosbach, K. Molecular Imprinting. *Trends Biochem. Sci.* **1994**, 19, 9-14.

(23) Vlatakis, G.; Andersson, L.I.; Müller, R.; Mosbach, K. Drug Assay Using Antibody Mimics Made by Molecular Imprinting. *Nature* **1993**, 361, 645-647.

(24) Aherne, A.; Alexander, C.; Payne, M.J.; Perez, N.; Vulfson, E.N. Bacteria-Mediated Lithography of Polymer Surfaces. J. *Am. Chem. Soc.* **1996**, 118, 8771-8772

(25) Alexander, C.; Vulfson, E.V. Spatially Functionalized Polymer Surfaces Produced via Cell-Mediated Lithography. *Adv. Mater.* **1997**, 9 (9), 751–755.

(26) Shi, H.; Tsai, W.B.; Garrison, M.D.; Ferrari, S.; Ratner, B.D. Template-Imprinted Nanostructured Surfaces for Protein Recognition. *Nature* **1999**, 398 (6728), 593–597.

(27) Dickert, F.L.; Hayden, O.; Halikias, K.P. Synthetic Receptors as Sensor Coating for Molecules and Living Cells. *Analyst* **2001**, 126 (6), 766–771.

(28) Hayden, O.; Dickert, F.L. Selective Microorganism Detection with Cell Surface Imprinted Polymers. *Adv. Mater.* **2001**, 13 (19), 1480–1483.

(29) Shen, X.; Bonde, J.S.; Kamra, T.; Bülow, L.; Leo, J.C.; Linke, D.; Ye, L. Bacterial Imprinting at Pickering Emulsion Interfaces. *Angew. Chem. Int. Ed.* **2014**, 53, 10687– 10690.

(30) Harvey, S.D.; Mong, G.M.; Ozanich, R.M.; Mclean, J.S.; Goodwin, S.M.; Valentine, N.B.; Fredrickson, J.K. Preparation and Evaluation of Spore-Specific Affinity-Augmented Bio-Imprinted Beads. *Anal. Bioanal. Chem.* **2006**, 386, 211-219.

(31) Cohen, T.; Starosvetsky, J.; Cheruti, U.; Armon, R. Whole Cell Imprinting in Sol-Gel Thin Films for Bacterial Recognition in Liquids: Macromolecular Fingerprinting. *Int. J. Mol. Sci.* **2010**, 11, 1236-1252.

(32) Ren, K.; Banaei, N.; Zare, R.N. Sorting Inactivated Cells Using Cell-Imprinted Polymer Thin Films. *ACS Nano* **2013**, 7, 6031-6036.

(33) Zhang, Z.; Guan, Y.; Li, M.; Zhao, A.; Ren, J.; Qu, X. Highly Stable and Reusable Imprinted Artificial Antibody Used for in situ Detection and Disinfection of Pathogens. *Chem. Sci.* **2015**, 6, 2822–2826.

(34) Tokonami, S.; Nakadoi, Y.; Takahashi, M.; Ikemizu, M.; Kadoma, T.; Saimatsu, K.; Dung, L.Q.; Shiigi, H.; Nagaoka, T. Label-Free and Selective Bacteria Detection Using a Film with Transferred Bacterial Configuration. *Anal. Chem.* **2013**, 85, 4925-4929.

(35) Hayden, O.; Mann, K.J.; Krassnig, S.; Dickert, F.L. Biomimetic ABO Blood-Group Typing. *Angew. Chem. Int. Ed.* **2006**, 45 (16), 2626–2629.

(36) Wangchareansak, T.; Thitithanyanont, A.; Chuakheaw, D.; Gleeson, M.P.; Lieberzeit, P.A.; Sangma, C. Influenza A Virus Molecularly Imprinted Polymers and their Application in Virus Sub-Type Classification. *J. Mater. Chem. B.* **2013**, 1, 2190–2197.

(37) Wang, Y.; Zhang, Z.; Jain, J.; Yi, J.; Mueller, S.; Sokolov, J.; Liu, Z.; Levon, K.; Rigas, B.; Rafailovich, M.H. Potentiometric Sensors based on Surface Molecular Imprinting: Detection of Cancer Biomarkers and Viruses. *Sens. Act. B – Chem.* **2010**, 146 (1), 381–387.

(38) Cai, D.; Ren, L.; Zhao, H.; Xu, C.; Zhang, L.; Ying, Y.; Wang, H.; Lan, Y.; Roberts, M.F.; Chuang, J.H.; Naughton, M.J.; Ren, Z.; Chiles, T.C. A Molecular-Imprint Nanosensor for Ultrasensitive Detection of Proteins. *Nat. Nanotechnol.* **2010**, 5, 597–601.

(39) Qi, P.; Wan, Y.; Zhang, D. Impedimetric Biosensor Based on Cell-Mediated Bioimprinted Films for Bacterial Detection. *Biosens. Bioelectron.* **2013**, 39, 282-288.

(40) Altintas, Z.; Gittens, M.; Guerreiro, A.; Thompson, K.; Walker, J.; Piletsky, S.; Tothill, I.E. Detection of Waterborne Viruses Using High Affinity Molecularly Imprinted Polymers. *Anal. Chem.* **2015**, 87 (13), 6801–6807.

(41) Altintas, Z.; Pocock, J.; Thompson, K.; Tothill, I.E. Comparative Investigations for Adenovirus Recognition and Quantification: Plastic or Natural Antibodies? *Biosens. Bioelectron.* **2015**, 74, 996–1004.

(42) Yilmaz, E.; Majidi, D.; Ozgur, E.; Denizli, A. Whole Cell Imprinting Based *Escherichia coli* Sensors: A Study for SPR and QCM. *Sens. Act. B. – Chem.* **2015**, 209, 714-721.

(43) van Grinsven, B.; Eersels, K.; Peeters, M.; Losada-Pérez, P.; Vandenryt, T.; Cleij, T.J.; Wagner, P. The Heat-Transfer Method: A Versatile Low-Cost, Label-Free, Fast and User-Friendly Readout Platform for Biosensor Applications. *ACS Appl. Mater. Interfaces* **2014**, 6, 13309-13318.

(44) Eersels, K.; van Grinsven, B.; Ethirajan, A.; Timmermans, S.; Jiménez Monroy, K.L.; Bogier, J.F.J.; Punniyakoti, S.; Vandenryt, T.; Hendriks, J.J.A.; Cleij, T.J.; Daemen, M.J.A.P.; Somers, V.; De Ceuninck, W.; Wagner, P. Selective identification of macrophages and cancer cells based on thermal transport through surface-imprinted polymer layers. *ACS Appl. Mater. Interfaces* **2013**, 5, 7258-7267.

(45) Bers, K.; Eersels, K.; van Grinsven, B.; Daemen, M.; Bogie, J.F.; Hendriks, J.J.; Bouwmans, E.E.; Püttmann, C.; Stein, C.; Barth, S.; Bos, G.M.; Germeraad, W.T.; De Ceuninck W.; Wagner, P. Heat-Transfer Resistance Measurement Method (HTM)-Based Cell

Detection at Trace Levels using a Progressive Enrichment Approach with Highly Selective Cell-Binding Surface Imprints. *Langmuir* **2014,** 30, 3631-3639.

(46) Eersels, K.; van Grinsven, B.; Khorshid, M.; Somers, V.; Püttmann, C.; Stein, C.; Barth, S.; Diliën, H.; Bos, G.M.J.; Germeraad, W.T.V.; Cleij, T.J.; Thoelen, R.; De Ceuninck, W.; Wagner, P. Heat-Transfer-Method-Based Cell Culture Quality Assay through Cell Detection by Surface Imprinted Polymers. *Langmuir* **2015**, 31, 2043-2050.

(47) Dickert, F.L.; Tortschanoff, M. Molecularly Imprinted Sensor Layers for the Detection of Polycyclic Aromatic Hydrocarbons in Water. *Anal. Chem.* **1999**, 71, 4559-4563.

(48) von Heijne, G. Membrane Protein Structure Prediction: Hydrophobicity Analysis and the Positive-inside Rule. *J. Mol. Bid.* **1992**, 225, 487-494.

(49) Gupta, R.S. Protein Phylogenies and Signature Sequences: A Reappraisal of Evolutionary Relationships Among Archaebacteria, Eubacteria, and Eukaryotes. *Microbiol. Mol. Biol. Rev.* **1998**, 62, 1435-1491.

Table of Content Figure